A Feasibility Study of 10MWh Class Energy Storage Flywheel System Using Superconducting Magnetic Bearing

Yajun ZHANG* , Kenzo NONAMI**, Hiromasa HIGASA***

*Dept. of Electronics and Mechanical Eng., Chiba University
**Dept. of Electronics and Mechanical Eng., Chiba University,
1-33 Yayoi-cho, Inage-ku, Chiba 263-8522, JAPAN
***Shikoku Research Institute Inc, 2109-8 Yashimanishi-machi, Takamatsu, Kagawa, Japan

INTRODUCTION

As difference of electric power required in day and night has been increasing, an energy storage and a smoothing of electric power in day and night become very important. If energy storage with high capacity could be able to realize, an efficiency of electric power system will become higher. An energy storage flywheel system using superconducting magnetic bearing is one of the most useful method of energy storage.

This paper is concerned with the feasibility study based on computer simulation to realize the 10MWh class energy storage flywheel system. Actually, we had done the exact vibration analysis of one model of 10MWh class flywheel rotor using CAE software based on a finite element method taking into account gyroscopic effect.

This flywheel system is the outer rotor which consists of a four spoke rib, CFRP flywheel, superconducting magnetic bearing(SMB) and active magnetic bearing(AMB). Conceptual design, vibration analysis, model used for control and control performance of the 10MWh class energy storage flywheel system are discussed in this paper in detail. Specially, We propose five kind of models to verify the stability of 10MWh class energy storage flywheel system with gyroscopic effect or not. The five kind of models are the ANSYS model with gyroscopic effect, the one-dimensional finite element mode(FEM) without gyroscopic effect, the FEM model with gyroscopic effect, the reduced-order model without gyroscopic effect and the flexible support model with gyroscopic effect. The FEM model is based on concept of the eigenvalue of FEM and the results of ANSYS analysis in the range of control(within 100Hz). The stablity of closed loop system was verified by these models. It is clarified that $H\infty$ controller taking into account gyroscopic effect can stabilize the flywheel system.

CONCEPTUAL DESIGN

A 10MWh class superconducting magnetic flywheel system for the electric power storage is shown in FIGURE 1 as a right-half cross-sectional view.

The position of AMB1, AMB2, AMB3, SMB and flywheel is shown in FIGURE 1. The total weight of the whole flywheel system is about 107t and the height is 6.86m. The weight of flywheel is approximately 45.7t and the diameter of the flywheel is 4.8m. The SMB is used to lift off the flywheel. In the system, the SMB is applied to both of the axial direction and the radial direction.

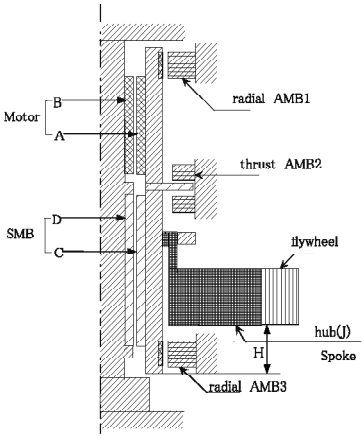

FIGURE 1: Cross sectional view of flywheel system

The main parameters of flywheel system are given in TABLE 1. The components of flywheel system are given in TABLE 2.

TABLE 1: Dimension of flywheel system

Structure parameter	Value[m]
Radius of stator	0.15
Radius of outer rotor	0.25
Radius of flywheel	2.40
Radius of spoke(aluminum)	0.36

Structure parameter	Value[m]
Axial direction length of flywheel	2.54
Span length of rotor	6.86
Height of spoke	1.72
Inner radius of flywheel	1.44
Inner radius of spoke	0.35
Radius of the steel ring	0.43
Axial direction height of steel ring	0.80
Height of flywheel(H)	0.50

TABLE 2: Function of flywheel system components

Flywheel	Mechancial energy storage
SMB	Lift off flywheel system
AMB1,AMB2 and AMB3	Control of system
Flywheel structure	Four spokes type
Rotational speed	6000rpm
Spring constant of SMB	$5.0 \times 10^9 N/m$

The control of this system is done with AMB arranged in the radial direction and the axial direction. The operational rotational speed of flywheel is 6000rpm. To reinforce the material of flywheel at the maximum speed of system, the material of CFRP is applied.

VIBRATION ANALYSIS

TABLE 3: Natural frequency of system when H(m) is varied

Rotion Speed	$H = 0.5$	$H = 1.0$	$H = 1.5$	$H = 2.0$
0.0Hz	25.4	26.8	27.5	24.7
	25.4	26.8	27.5	24.7
	89.2	62.9	62.5	74.6
	89.2	62.9	62.5	74.6
30.0(Hz)	22.1	26.4	27.3	23.0
	28.8	28.7	27.7	23.0
	81.5	55.4	49.7	61.4
	97.4	78.2	77.1	90.5
60.0(Hz)	18.9	24.5	27.1	21.1
	31.7	29.4	27.8	27.1
	75.1	47.5	39.8	51.8
	105.1	90.1	91.5	106.8
90.0(Hz)	16.2	22.3	26.7	18.9
	34.2	29.9	27.9	28.8
	70.1	42.4	32.6	45.2
	111.5	100.3	103.7	120.8
120.0(Hz)	13.9	19.8	25.1	16.9
	36.3	30.4	28.8	28.8
	66.3	39.3	28.6	41.1
	116.7	108.3	113.1	126.4

We carried out the vibration analysis of flywheel system by ANSYS which is a kind of CAE software based on finite element method. After constructing the three dimensional model of flywheel system with gyroscopic effect, the eigenvaule and eigenvector were computed by ANSYS. The detailed vibration analysis was done with gyrosopic effect. But the influences of SMB and AMB are ignored.
The eigenvalue of flywheel system changed with gyrosopic effect including paratmeter H is given in TABLE 3. H is the hegiht of flywheel from bottom as shown in FIGURE 1. The relation between rotation speed and eigenvalue with gyroscopic effect is given in FIGURE 2 when H is 0.5m.

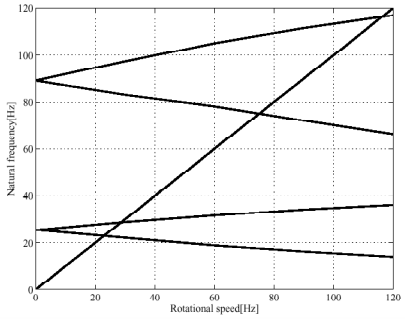

FIGURE 2: Relations between natural frequency and rotational speed(H=0.5m)

From the result of ANSYS , it is clarified there is the first flexible mode(28.5Hz) in the range of control(with 100Hz) with gyroscopic effect. By adaptive vibration control using frequency estimation, we can control the vibration of the system passing through it's critical speed.

ONE-DIMENSIONAL FEM MODEL WITHOUT GYROSCOPIC EFFECT AND SIMULATION

There are three AMB's in the system to control the system against a sudden disturbance and to pass it's critical speeds. The SMB is needed for lift off the weight of flywheel system. In order to construct the model of system with the effects of SMB, AMB and coreless motor, the system is divided into ten parts. The one-dimensional FEM model is given in FIGURE.3.

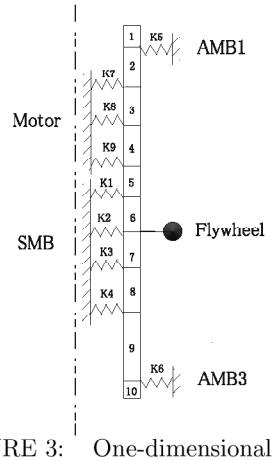

FIGURE 3: One-dimensional FEM model

The position of AMB1, AMB3, SMB, motor and flywheel are shown in FIGURE 3. $x_1, x_2, x_3, ..., x_{10}$ are the displacements of each position. AMB2 is used for the control of the axial direction. AMB1 and AMB3 are used for the control of the radial direction. One example of ANSYS analysis is given in FIGURE 4.

Based on FIGURE 3, the condition and output equation of the flywheel are computed. Supposes X, Y direction are same, and only X direction is taken into consideration. We can get one-dimensional FEM model by free-free flywheel system as follows:

$$M\ddot{X} + KX = 0 \tag{1}$$

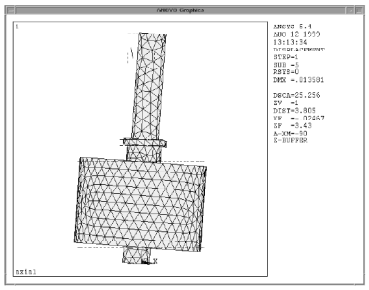

FIGURE 4: Example of ANSYS analysis (Case of rigid mode)

Here, $X = [x_1 \quad \theta_1 \quad x_2 \quad \theta_2 \quad \cdots \quad \theta_{10} \quad x_{11} \quad \theta_{11}]^T$, M is mass matrix, K is stiffness matrix. TABLE 4 shows the comparison ANSYS analysis with one-dimensional FEM analysis. The results of ANSYS analysis is close to that of one dimensional FEM model in TABLE 4. The one-dimensional FEM analysis is computed with effect of SMB and AMB.

TABLE 4: Results of ANSYS and one-dimensional FEM model (Hz)

	ANSYS	One-dimensional FEM
1st rigid mode	0	0.20
2nd rigid mode	0	4.25
1st flexible mode	25.4	32.03
2nd flexible mode	89.2	151.3

The two rigid modes of flywheel system are zero computed by ANSYS because SMB and AMB are ignored. The mode shape which computed by Eq.(1) is given in FIGURE 5. FIGURE 5(a) is the first natural mode and (b) is the second natural mode. In FIGURE 5, the position 5 is the place of flywheel. Because the weight of flywheel and auxiliary component are about 100t, the displacement of position 5 is close to zero.

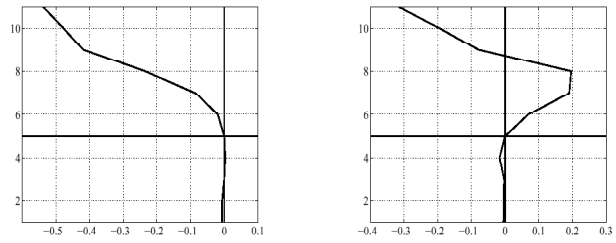

(a) First flexible mode (32.03Hz) (b) Second flexible mode (151.38Hz)

FIGURE 5: Flexible mode of system

The control inputs are at the place of AMB1 and AMB3. The equation of motion of flywheel system with control input and disturbance input is given as follows:

$$M\ddot{X} + KX = FU \quad EW \tag{2}$$

IIere F is the matrix used for the control input and E is used for disturbance. If the disturbance is the place of flywheel, the E is the matrix which only value is 1 at line 13. The displacements of AMB1 and AMB3 can be measured because the gap sensors are arranged each place of AMB1 and AMB3.
From Eq.(2), we can construct the reduced-order model used for control. The reduced-order model used for control is made to truncate the high vibration mode in the model coordinate. The reduced-order model used for control is made by the one-dimensional FEM model with two rigid modes and one flexible mode. The reduced-order model is given as follows:

$$\begin{cases} \dot{x_r} = A_r x_r + B_r u + E_r w \\ y_r = C_r x_r + D_r U \end{cases} \tag{3}$$

Where, $A_r \in R^{6\times6}$ $B_r \in R^{6\times2}$ $E_r \in R^{6\times1}$ $C_r \in R^{2\times6}$ $D_r \in R^{2\times2}$ $x_r \in R^{6\times1}$ $y_r \in R^{2\times1}$ $u \in R^{2\times1}$ $w \in R^{1\times1}$ The reduced-order model is used to design the $H\infty$ controller.
$H\infty$ control is to minimize a certain cost function(γ) defined in the frequency domain. This cost function is described with the following $H\infty$ norm.

$$\|G(s)\|_\infty = sup\sigma\,\{G(j\omega)\} \tag{4}$$

σ is a maximum singular value $G(j\omega)$. $H\infty$ control decides the controller K which could stablize the closed loop by the feedback control of $u = Ky$ to the augumented plant. The augumented plant is given in FIGURE 6. FIGURE 6 is used for the reduced-order model of Eq.(3).

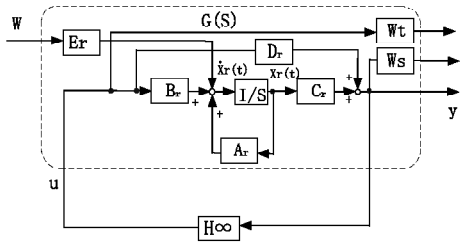

FIGURE 6: Augumented plant and $H\infty$ cotrol

In FIGURE 6, A_r, B_r, C_r, D_r, E_r are the matrices of the reduced-order model. u is the control input. y is the measured output. W is the noise. W_s and W_t are the weighting functions. Then, the designed controller is used to actual system and verify that the controller doesn't cause spillover phenomenon in

the closed loop of the actual system. The weighting functions W_s and W_t used for controller are shown in FIGURE 7.

The simulation is done by using $H\infty$ control to the model indicated from Eq.(2) and examines the characteristic value of the closed loop. FIGURE 8 is the impulse disturbances response (Maximum value is 100N). The upper figure (a) is the output of AMB1. The bottom figure (a) is the output of AMB3. (b) is the control input.

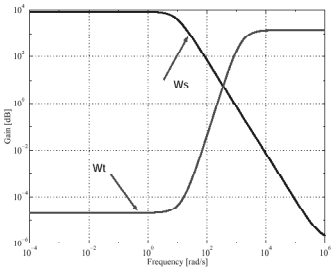

FIGURE 7: Weighting functions W_s and W_t

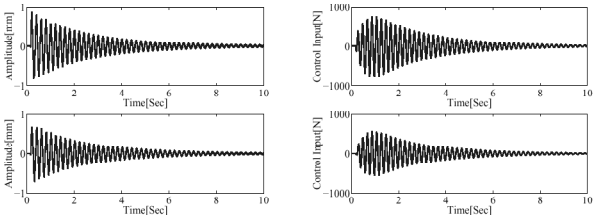

(a) Displacement (b) Control input

FIGURE 8: Impulse disturbances responses

FIGURE 9 is the initial value responses. The initial value of the system is $2mm$ on the touchdown bearing.

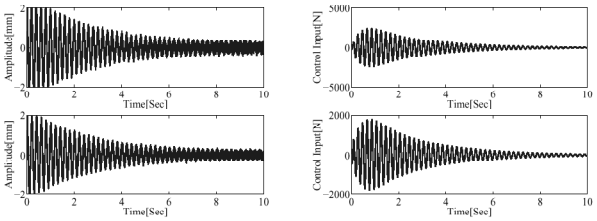

(a) Displacement (b) Control input

FIGURE 9: Responses with initial valuc(touchdown 2mm)

LOW DIMENSIONAL MODEL WITH GYROSCOPIC AND SIMULATION

For FIGURE 3, one-dimensional FEM model based equation of motion with gyroscopic effect can be written as follows.

$$M\ddot{Z} + G\dot{Z} + KZ = 0 \qquad (5)$$

The dimensions of M, G, K become two times of Eq.(1). G is gyroscopic matrix. Z is $Z = [X, Y]^t$.

The spring constants of the AMB and the SMB are concered with Eq.(5).

In order to get the reduced-order model of Eq.(5), the mode separate must be done as same as reduce-order model without gyroscopic effect. The modal separation for Eq.(5) is very complicated because gyroscopic matrix exist and the mode separate must be done in the plural domain.

Therefore the low dimensional model with gyrospic effect is taken into account. The low-dimensional model of FIGURE 10 is introdued as rotation shaft model with flexible support and gyroscopic effect in this chapter. Before an introduction, we assume: (1)A rotor is a flexible body, and the mass of the rotor can be ignored. (2)The rotor do a movement only in xy plane.

For FIGURE 10, the following equation of motion with gyroscopic effect can be obtained. Here, we only consider the rotational speed of the system. The acceleration of system is ignored.

$$m\ddot{x_0} + \alpha(x_0 - X) + \gamma(\theta_x - k_x) = 0$$

$$m\ddot{y_0} + \alpha(y_0 - Y) + \gamma(\theta_y - k_y) = 0$$

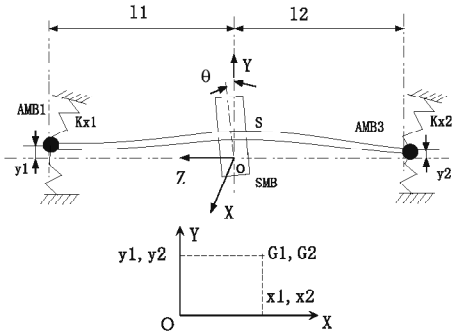

FIGURE 10: Rotation shaft model with flexible support and gyroscopic effect

$$I\ddot{\theta}_x - I_p\omega\dot{\theta}_y + \gamma(x_0 - X) + \delta(\theta_x - k_x) = 0$$

$$I\ddot{\theta}_y + I_p\omega\dot{\theta}_x + \gamma(y_0 - Y) + \delta(\theta_y - k_y) = 0$$

Here,

$$\mathrm{X} = \begin{pmatrix} x_0 & y_0 & \theta_x & \theta_y \end{pmatrix}^{\mathrm{T}} \quad \mathrm{U} = \begin{pmatrix} x_1 & y_1 & x_2 & y_2 \end{pmatrix}^{\mathrm{T}}$$

$$\mathrm{M} = \begin{pmatrix} m & 0 & 0 & 0 \\ 0 & m & 0 & 0 \\ 0 & 0 & I & 0 \\ 0 & 0 & 0 & I \end{pmatrix} \mathrm{G} = \begin{pmatrix} 0 & 0 & 0 & 0 \\ 0 & 0 & 0 & 0 \\ 0 & 0 & 0 & -I_pW \\ 0 & 0 & I_pW & 0 \end{pmatrix}$$

$$k_x = \frac{x_2 - x_1}{l} \quad k_y = \frac{y_2 - y_1}{l} \quad X = \frac{l_2x_1 + l_1x_2}{l}$$

$$\mathrm{Y} = \frac{\mathrm{l_2y_1 + l_1y_2}}{\mathrm{l}} \mathrm{K} = \begin{pmatrix} \alpha & 0 & \gamma & 0 \\ 0 & \alpha & 0 & \gamma \\ \gamma & 0 & \delta & 0 \\ 0 & \gamma & 0 & \delta \end{pmatrix} \mathrm{C} = \begin{pmatrix} 1 & 0 \\ 0 & 1 \\ 0 & 0 \\ 0 & 0 \end{pmatrix}^{\mathrm{t}}$$

TABLE 5: Nomenclature

I	Diametral moments of inertia
I_p	Polar moments of inertia
K_{x1} K_{x2}	Equivalent spring constant in horizontal
K_{y1} K_{y2}	Equivalent spring constant in vertical
l	Length of rotor($l = l_1 + l_2$)
l_1 l_2	Distance
m	Mass of rotor
α	Stifness constant in deflection
δ	Stifness constant in inclination
γ	Influence cofficient between α and δ
θ	Inclination angle of rotor
θ_x θ_y	Components of rotation angle
ω	Angular velocity

Using the above equation, the equations of motion can be written as:

$$\begin{cases} M\ddot{X} + G\dot{X} + KX = BU \\ Y = CX \end{cases} \tag{6}$$

From Eq.(6), the state-space equations of system can be written as:

$$\begin{cases} \dot{x_g} = A_g x_g + B_g u_g + E_g w_g \\ y_g = C_g x_g + D_g u_g \end{cases} \tag{7}$$

Where, $A_g \in R^{8\times8}$ $B_g \in R^{8\times4}$ $E_g \in R^{8\times2}$ $C_g \in R^{2\times8}$ $D_g \in R^{2\times4}$ $x_g \in R^{8\times1}$ $y_g \in R^{2\times1}$ $u_g \in R^{4\times1}$ $w_g \in R^{2\times1}$ Eq.(7) is used as model for controller design. The augumented plant of the system is as same as FIGURE 6. A_g, B_g, E_g, C_g, D_g are substituted for A_r, B_r, E_r, C_r, D_r in FIGURE 6. The dimensions of u_g, w_g are two times of FIGURE 6. The rotating shaft model with flexible support and gyroscopic effect is used for $H\infty$ controller design. The weighting functions to control the flexible mode in FIGURE 10 are shown in the following figure.

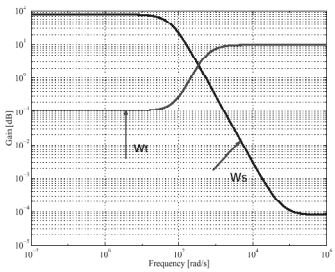

FIGURE 11: Weighting functions W_s and W_t

In order to verify the validity of controller designed in FIGURE 11, the controller is put into closed loop system of Eq.(5). The performance of closed loop was examined to verfiy the stability of closed loop system with the parmater of the rotational speed ω.

From the result of simulation, the $H\infty$ controller designed in FIGURE 11 can stablize the closed loop system in all rotating speed range.
Because the dimension of closed loop with gyroscopic effect system is very high, it is impossible to do the proper numerical calculation of disturbance responses for the closed loop. So, after the characteristic value anslysis and the stability of the above mentioned closed loop was evaluated, the closed loop disturbance responses by the low-dimensional model of the FIGURE 10 was carried out.
The initial value responses are given in FIGURE 12. The upper figure (a) is the output of X direction of flywheel, and the bottom figure (a) is Y direction. (b) shows the control input of the X direction of AMB1, the X direction of AMB3, the Y direction of AMB1, the Y direction of AMB3.

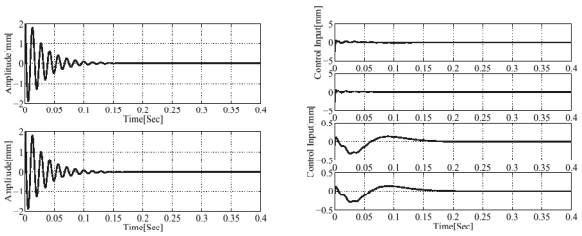

(a) Displacement (b) Control input

FIGURE 12: Responses with initial value(touchdown 2mm)

The impulse disturbances responses are given in FIGURE 13. The maximum value of disturbances is 100N.

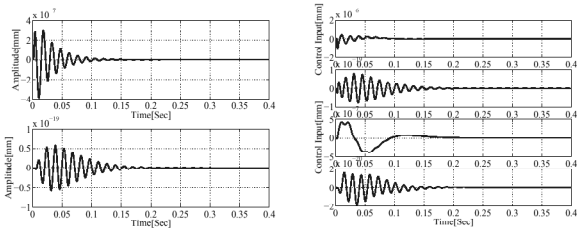

(a) Displacement (b) Control input

FIGURE 13: Impulse disturbances responses (Rotating Speed is 0Hz)

The impluse disturbance to x direction of flywheel is added, the impulse disturbances response at rotating speed 120Hz is shown in FIGURE 14.

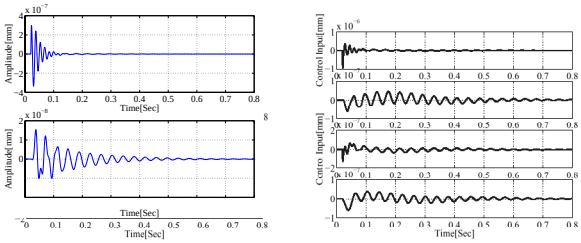

(a) Displacement (b) Control input

FIGURE 14: Impulse disturbances responses (Rotating speed is 120Hz)

From FIGURE 13 and FIGURE 14, we see there is vibration at rotational speed $\omega = 120Hz$. This is because $H\infty$ controller is designed by condition of $\omega = 0Hz$. The vibration can be constrained if $H\infty$ controller is designed at $\omega = 120Hz$. After all, the control of gyroscopic of gain scheduled[5] is suitable. Beacuse energy storage flywheel rotor has strong gyroscopic effect, it is important how to make the low-dimensional model with gyroscopic effect used for controller design. Moreover, how to examine the appropriate of controller for the closed loop system is important. The paper gives a new method to construct low-dimensional model with gyroscopic effect and verified the stablity of high dimensional model with gyroscopic effect. From simulation, we see the method is useful for flywheel system.

CONCLUSION

This paper is concerned with the feasibilty stduy of the 10MWh class superconductivity magnetic bearing flywheel system. The vibration analysis by ANSYS with gyroscopic effect, one-dimensional FEM models of flywheel system with and without gyroscopic effect, reduced-order model, low-dimensional model with gyroscopic effect and $H\infty$ controller design were disscued in this paper. From the simulation, the following conclusions can be obtained.

The eigenvaule and eigenvector were computed by ANSYS analysis. From the result of vibration analysis, it is confirmed that there is the first flexible mode in the range of control. But the vibration of system passing through it's critical speed can be controlled by adaptive vibration control.

We designed one-dimensional FEM models with and without gyroscopic effect. Using one-dimensional FEM model without gyroscopic effect, we can construct the reduced-order model by mode separation which used for control. But the mode separation is very complicated for one-dimensional FEM model with gyroscopic effect because gyroscopic matrix exist. We introduced low-dimensional model of rotating shaft model with flexible support and gyroscopic effect for control. Using this model, we desiged the $H\infty$ controller for high-dimensional system. But it is not possible to compute the disturbance responses of the closed loop beacuse the dimension of system is very high. For this reason, we verified the stablity of the closed loop system by eigenvalue analysis of closed loop system. From the results, it is found the system is controllable.

Three AMB's were used to control the system against a sudden disturbance and to passing throught it's critical speeds. We designed the controller used for AMB by models with or without gyroscopic effect. From the simulation, we see if controller was designed by model without gyroscopic effect, it can not control the closed system with gyroscopic effect. But if the controller was designed by model with gyroscopic effect, it can control the closed system with gyroscopic effect.

This paper proposal a new concept how to compute low-dimensional model with gyroscopic effect and how to verfiy the controllbility of the closed loop system. It is clarified the method is useful for flywheel system.

The future research is to check the general structure and redesign the parameter.

References

[1] Y.Miyamgawa,H.Kameno,R.Takahata and H.Ueyama,A 0.5KWh Flywheel Energy Storage System Using A IIigh-Tc Superconducting Magnetic Bearing, Preprint of ASC'98 in Palm Springs,CA,September 17,1998

[2] Hans J.Bornemann Conceptual System Design of a 5MWh/100MW Superconducting Flywheel Energy Storage Plant for Power Utility Application IEEE Transactions On Applied Superconducting,Vol.7, NO.2,pp.398-401,JUNE 1997

[3] Z,xia Q Y chen K B Ma C K McMichael M Lamb R s Cooley P C Flowler and W K Chu Design of Superconducting Magnetic Bearing with High Levitating Force for Flywheel Energy Storage Systems IEEE Transactions on Applied Super- conductivity,Vol.5.No.2,pp.622-625,June 1995

[4] Krwin kramer,Dynamics of Rotors and Foundation, Springer-Verlag(1993)

[5] Selim,S, Nonami,K, Gain-Scheduled ∞ Control of Active magnetic Bearing Systems with Gyroscpic Effect Trans.JSME.Ser.C,63,pp.120-127(1996)

[6] ZiHe-Liu,Nonami,K, Adaptive Vibration Control Using Frequency Estimation For Multipe Peridic Disturbances with Adaptive Frequency Tracking Trans.JSME.Ser.C 65(638),4305-4311(1999)

[7] Yajun Zhang, Kenzo Nonami, Hiromasa Higasa, Feasibility Study of Modeling and Control for 10MWh Class Energy Storage Flywheel System Using Superconduting Magnetic Bearing Proceedings of the 12th International Symposium on Supercondutivity,(1999),803-805